

RESEARCH ARTICLE | AUGUST 13 2024

# Low-temperature growth of high-quality VO<sub>2</sub> epitaxial film on c-plane sapphire by reactive magnetron sputtering


Chang Liu ; Zhi Zheng ; Xing Li; Yang Wang; Xiang Dong ; Gaoshan Huang ; Yongfeng Mei  


 Check for updates


*Appl. Phys. Lett.* 125, 071904 (2024)


<https://doi.org/10.1063/5.0219061>




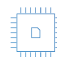
  
Nanotechnology & Materials Science


  
Optics & Photonics

  
Impedance Analysis

  
Scanning Probe Microscopy


  
Sensors

  
Failure Analysis & Semiconductors



**Unlock the Full Spectrum.**  
From DC to 8.5 GHz.  
Your Application. Measured.

[Find out more](#)



# Low-temperature growth of high-quality VO<sub>2</sub> epitaxial film on c-plane sapphire by reactive magnetron sputtering

Cite as: Appl. Phys. Lett. **125**, 071904 (2024); doi: 10.1063/5.0219061

Submitted: 15 May 2024 · Accepted: 31 July 2024 ·

Published Online: 13 August 2024



View Online



Export Citation



CrossMark

Chang Liu,<sup>1</sup>  Zhi Zheng,<sup>1</sup>  Xing Li,<sup>1</sup> Yang Wang,<sup>1</sup> Xiang Dong,<sup>1</sup>  Gaoshan Huang,<sup>1,2,3</sup>   
and Yongfeng Mei<sup>1,2,3,4,a)</sup> 

## AFFILIATIONS

<sup>1</sup>Department of Materials Science and State Key Laboratory of Molecular Engineering of Polymers, Fudan University, Shanghai 200438, People's Republic of China

<sup>2</sup>Yiwu Research Institute of Fudan University, Yiwu, Zhejiang 322000, People's Republic of China

<sup>3</sup>International Institute of Intelligent Nanorobots and Nanosystems, Fudan University, Shanghai 200438, People's Republic of China

<sup>4</sup>Shanghai Frontiers Science Research Base of Intelligent Optoelectronics and Perception, Institute of Optoelectronics, Fudan University, Shanghai 200438, People's Republic of China

<sup>a)</sup> Author to whom correspondence should be addressed: [yfm@fudan.edu.cn](mailto:yfm@fudan.edu.cn)

## ABSTRACT

The growth of VO<sub>2</sub> epitaxial films has been researched extensively for obtaining excellent phase-transition performance. However, previous methods typically necessitate high temperatures or post-annealing processes, which elevate both experimental complexity and cost. In this work, we prepared high-quality VO<sub>2</sub> epitaxial films by reactive magnetron sputtering directly under a low growth temperature. Benefiting from the determination of the oxygen pressure ratio from the theoretical analysis of the sputtering process model, single-stoichiometric VO<sub>2</sub> epitaxial films could be prepared under 450 °C with a resistance change of 10<sup>3</sup>, and above 500 °C with a resistance change exceeding 10<sup>4</sup>. The mechanism of achieving low-temperature growth of VO<sub>2</sub> epitaxial films was analyzed utilizing Thornton's zone model; finally, the epitaxial characteristics of VO<sub>2</sub> on the sapphire substrate were confirmed from in-plane and out-of-plane directions. This work presents a guideline for the low-temperature growth of VO<sub>2</sub> epitaxial films with enhanced phase-transition performance, thereby reducing both the cost and the requirements associated with the epitaxial growth of VO<sub>2</sub> films.

Published under an exclusive license by AIP Publishing. <https://doi.org/10.1063/5.0219061>

VO<sub>2</sub> has become one of the most popular strongly correlated materials due to its profound physical mechanisms and various changes in physical properties during the phase transition.<sup>1</sup> Around 340 K, it undergoes the metal-insulator transition (MIT), accompanied by a structural phase transition from the low-temperature monoclinic phase (P21/c) to the high-temperature tetragonal rutile phase (P42/mnm). The physical properties of VO<sub>2</sub> films such as electrical resistance,<sup>2–4</sup> optical transmittance,<sup>5</sup> and macroscopic volume<sup>6</sup> exhibit changes across the MIT, which can be triggered by various stimuli.<sup>7–10</sup> Utilizing these properties, various novel devices such as microelectromechanical devices,<sup>11,12</sup> infrared detector,<sup>13,14</sup> camouflage,<sup>15</sup> and actuator<sup>16–18</sup> have been widely studied. The performance of advanced VO<sub>2</sub> devices critically depends on film quality, and compared with polycrystalline VO<sub>2</sub>, the epitaxial VO<sub>2</sub> can further enhance the MIT property. However, the preparation of pure stoichiometric VO<sub>2</sub> epitaxial films

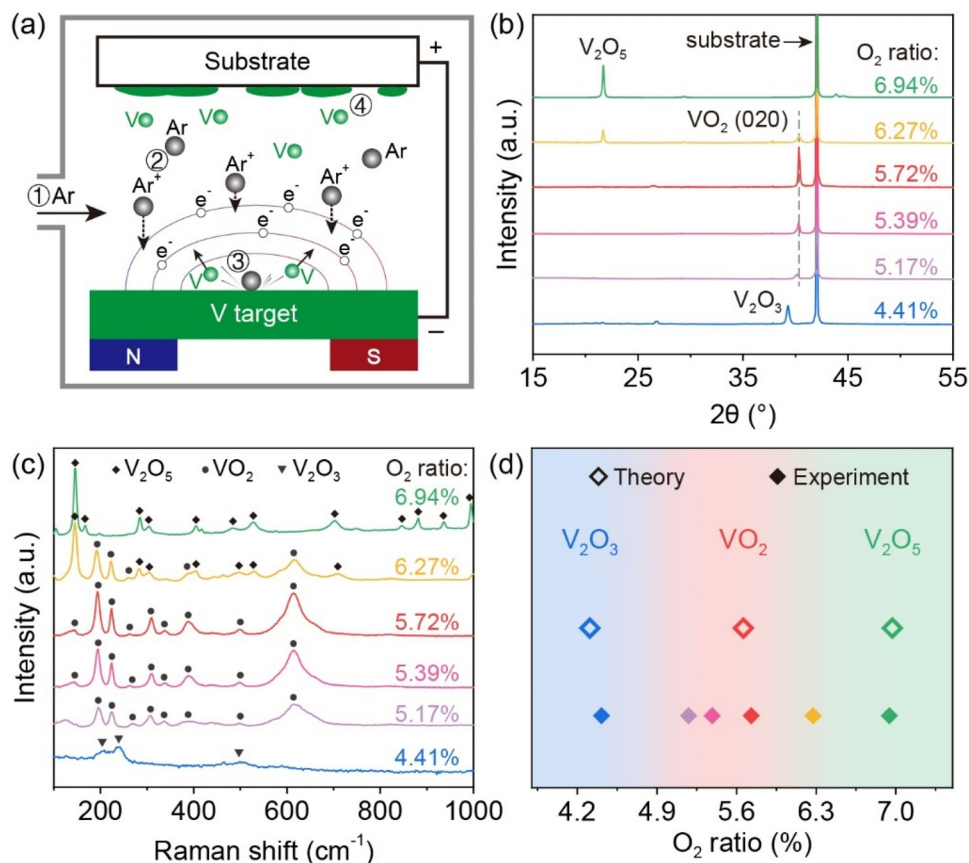
has been a significant challenge due to vanadium oxides being sensitive to oxygen, and the growth usually needs high temperature.<sup>19,20</sup>

Various techniques have been used to grow VO<sub>2</sub> epitaxial films.<sup>21–24</sup> For instance, a VO<sub>2</sub> epitaxial film was prepared using RF-plasma assisted oxide molecular beam epitaxy (MBE) under 550 °C, which had a third-order-of-magnitude resistance change ( $\Delta R$ ) across the MIT.<sup>23</sup> It could also be grown under 400 °C by MBE and post-annealing, but the  $\Delta R$  was only 25.<sup>24</sup> Pulsed laser deposition is often employed for the preparation of VO<sub>2</sub> epitaxial films as well.<sup>25,26</sup> Under the growth temperature of 600 °C, a VO<sub>2</sub> epitaxial film was grown on sapphire, showing fourth-order-of-magnitude  $\Delta R$ .<sup>26</sup> In addition, for producing high-quality and large-scale thin films, the sputtering technique has proven to be an efficient method.<sup>27–29</sup> The published works employed ion-beam sputtering,<sup>30,31</sup> DC, or RF-sputtering.<sup>32–34</sup> Among them, an epitaxial VO<sub>2</sub> film was prepared under the growth

temperature of 590 °C, demonstrating a high  $\Delta R$  of  $10^4$  and infrared modulation of 50%.<sup>35</sup> Some work also attempted to grow VO<sub>2</sub> films below 400 °C, but the polycrystalline nature of VO<sub>2</sub> only allows for a three-order-of-magnitude change in resistance.<sup>36</sup> Additional treatments such as post annealing,<sup>37</sup> substrate bias,<sup>38</sup> and seed layer<sup>39</sup> were often required. Until now, there is still a lot of work dedicated to growing high-quality VO<sub>2</sub> epitaxial films using magnetron sputtering. However, most of them require high growth temperatures even reaching up to 650 °C<sup>40</sup> or post-annealing treatments.<sup>33,41</sup>

In this study, we realize the growth of the VO<sub>2</sub> epitaxial film by reactive magnetron sputtering under growth temperature as low as 450 °C through systematically investigating the growth conditions. With the help of the sputtering process model, the theoretical oxygen pressure ratios required for the formation of VO<sub>2</sub> was analyzed, and different stoichiometric vanadium oxides were prepared in the experiment according to the theoretical condition. Based on the obtained precise oxygen pressure ratio, a single-stoichiometric VO<sub>2</sub> film was grown on a sapphire substrate under different growth temperatures. Subsequently, the nanomembrane quality was characterized by x-ray diffraction (XRD), Raman spectroscopy, and temperature-dependent resistance measurements, confirming the property and epitaxial relation with the sapphire substrate of a VO<sub>2</sub> film.

For preparation of a VO<sub>2</sub> film by magnetron sputtering, a metal vanadium target and a DC power of 200 W were utilized under a background vacuum of  $E^{-6}$  Torr. The influence of O<sub>2</sub> pressure ratio was initially investigated using argon (Ar) as the working gas at a fixed pressure of 13 mTorr. To determine the O<sub>2</sub> pressure ratios for VO<sub>2</sub> growth, the sputtering process model is established as shown in Fig. 1(a).<sup>42</sup> There are mainly four steps during the growth: gas injection, Ar ionization, sputtering V atoms, and V reacting with O<sub>2</sub>. When a specific pressure of Ar is introduced, determining the amount of O<sub>2</sub> required to obtain VO<sub>2</sub> can be achieved by estimating the quantity of V atoms involved in the reaction through the two intermediate steps. (i.e., Ar ionization and sputtering V atoms). The ionization efficiency is used to describe how much Ar can be ionized into Ar<sup>+</sup> to bombard the V target. According to previous reports, the ionization efficiency of Ar in our experiment is approximately 60%.<sup>43,44</sup> Moreover, when an Ar<sup>+</sup> bombards the V target, the amount of V atoms that can be sputtered out is called the sputtering yield.<sup>45</sup> Based on the applied DC power and gas pressure, the estimated sputtering yield of V atoms is approximately 10%.<sup>46,47</sup> As a result, the number of sputtered V atoms can be calculated according to the Ar pressure introduced. Assuming the sticking coefficient is approximately 1, meaning all sputtered V atoms can react with O<sub>2</sub>,<sup>48</sup> the theoretical O<sub>2</sub> ratios required to



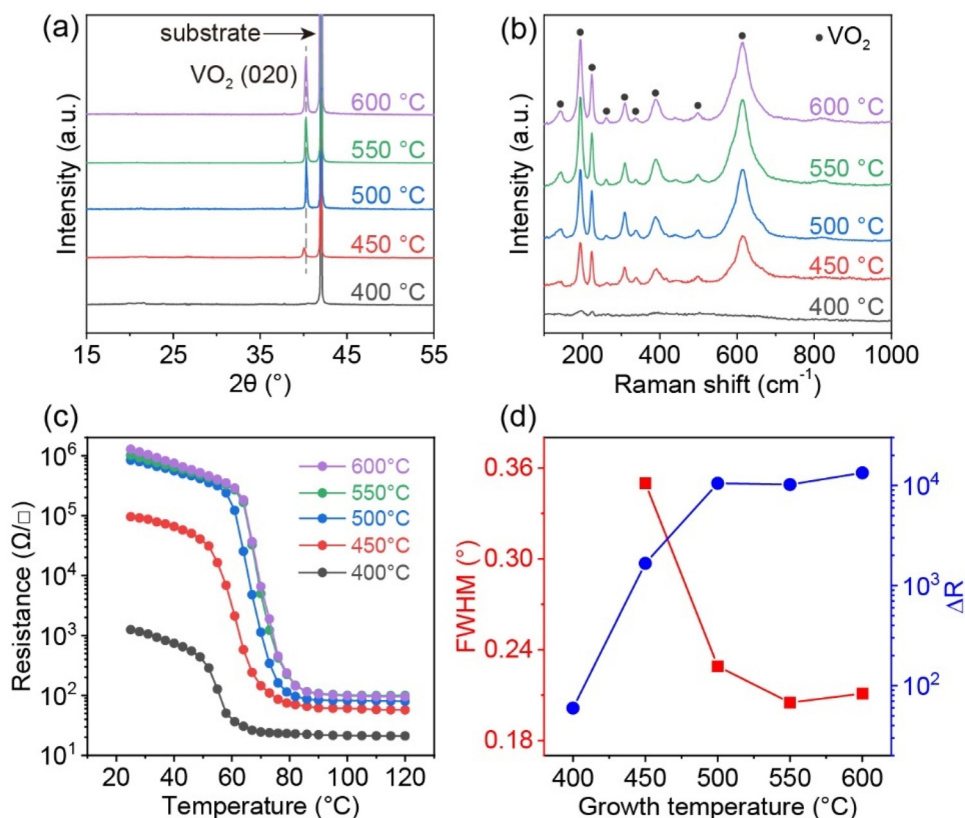
**FIG. 1.** The effect of O<sub>2</sub> pressure ratio on the formation of vanadium oxides. (a) Schematic diagram of the sputtering growth process of the vanadium oxide film. (b) XRD  $2\theta$ - $\omega$  curves of vanadium oxide films under different O<sub>2</sub> pressure ratios. (c) Raman spectroscopies of vanadium oxide films under different O<sub>2</sub> pressure ratios. (d) Major phases of sputtered vanadium oxides as a function of O<sub>2</sub> pressure ratios.

produce  $V_2O_3$ ,  $VO_2$ , and  $V_2O_5$  were calculated to be 4.31%, 5.66%, and 6.97%, respectively.

According to the calculation, we varied the  $O_2$  pressure to 0.6, 0.71, 0.74, 0.79, 0.87, and 0.97 mTorr, and the proportion of  $O_2$  under the total pressure was 4.41%, 5.17%, 5.39%, 5.72%, 6.27%, and 6.94%, respectively. The XRD  $2\theta$  curves shown in Fig. 1(b) are to detect structures of vanadium oxide films obtained at different  $O_2$  ratios. It can be observed that when the  $O_2$  ratio is 4.41%, the vanadium oxide film mainly exhibits diffraction peaks of  $V_2O_3$ , indicating insufficient  $O_2$  content and the formation of low-valence state vanadium oxides. With the  $O_2$  ratio increasing to 5.17%, the weak  $VO_2$  (020) diffraction peak indicates the formation of the  $VO_2$  phase. Subsequently, the  $VO_2$  diffraction peak intensity gets stronger as the  $O_2$  ratio increases, reaching its maximum when the  $O_2$  ratio reaches 5.72%. However, further increasing  $O_2$  ratio to 6.27% results in the coexistence of  $VO_2$  and  $V_2O_5$  phases, indicating that excessive  $O_2$  oxidizes part of the  $VO_2$  to the higher valence state  $V_2O_5$ , and the  $O_2$  ratio of 6.94% leads to the formation of  $V_2O_5$  completely. Raman spectroscopy is also utilized to confirm the phases of vanadium oxides shown in Fig. 1(c), and the results show that the phases corresponding to the Raman vibrational peaks are consistent with the XRD results. By comparing the results in the experiment and in theory in Fig. 1(d), it can be concluded that the

experimental results are basically consistent with the theoretical predictions.

Upon determining the  $O_2$  pressure ratio required for  $VO_2$  growth, it is advantageous for investigating the growth temperature's influence because we only need to consider the growth temperature's effect on the crystalline quality of  $VO_2$  film, without having to account for compositional deviations. Thus,  $VO_2$  films were grown at a series of temperatures, including 400, 450, 500, 550, and 600 °C under optimized gas environment conditions. The structure and phase of  $VO_2$  films obtained under various growth temperatures are checked using XRD and Raman spectroscopy. As shown in Fig. 2(a), XRD  $2\theta$  curves illustrate that no diffraction peaks are detected at 400 °C, indicating that 400 °C is too low to be favorable for the crystallization of a  $VO_2$  film. Subsequently, as the growth temperature increases to 450 °C, the  $VO_2$  (020) plane diffraction peak appears, which means the realization of the epitaxial growth. Furthermore, the intensity of diffraction peak becomes stronger, indicating that higher temperature promotes the crystallization of  $VO_2$  films, resulting in a significant improvement in film quality. Although all the Raman peaks in the Raman spectra in Fig. 2(b) belong to the monoclinic phase of  $VO_2$ , the peak intensity of  $VO_2$  film grown at 400 °C is weaker than that of  $VO_2$  films grown above 450 °C, showing the same trend as the XRD results.

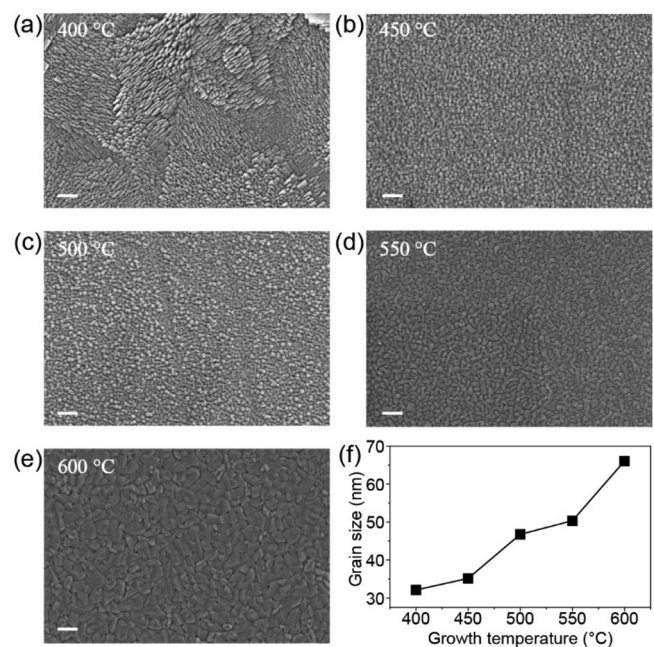


**FIG. 2.** The effect of growth temperature on  $VO_2$  films. (a) XRD  $2\theta$ - $\omega$  curves of  $VO_2$  films grown under different growth temperatures. (b) Raman spectroscopies of  $VO_2$  films grown under different growth temperatures. (c) Temperature-dependent electrical resistance of  $VO_2$  films grown under different growth temperatures. (d) FWHM of XRD diffraction peaks and  $\Delta R$  of  $VO_2$  films as the variation of growth temperatures.

The electrical MIT properties are also characterized by temperature-dependent resistance curves as shown in Fig. 2(c). When the growth temperature is 400 °C, the film shows  $\Delta R$  of  $\sim 59$  during the heating process, indicating a poor crystallization of the VO<sub>2</sub> film. The temperature-dependent resistance curve changes steeper during the phase transition when the growth temperature of VO<sub>2</sub> film is 450 °C, and the  $\Delta R$  is  $\sim 10^3$ , which is comparable to the electrical MIT performance of most VO<sub>2</sub> thin films.<sup>20,33,41,49,50</sup> It is already feasible to achieve the fabrication of good VO<sub>2</sub> epitaxial films at 450 °C. Further increasing the growth temperature to 500, 550, and 600 °C, the MIT phenomenon gets further enhanced with the  $\Delta R$  of  $\sim 10^4$ , which is the benchmark of high quality for a VO<sub>2</sub> epitaxial film.<sup>2,3,51,52</sup> By comparing the FWHM of XRD peaks and the  $\Delta R$ , as shown in Fig. 2(d), it can be seen that both the crystalline quality and the  $\Delta R$  during the MIT increase with increasing growth temperature from 400 to 500 °C, and they remain relatively constant above 500 °C.

To get a deeper understanding of why epitaxial growth of VO<sub>2</sub> films can be realized under lower growth temperatures, we analyze the grain morphology with the help of Thornton's zone model. The scanning electron microscope (SEM) images of VO<sub>2</sub> films grown under different growth temperatures are shown in Figs. 3(a)–3(e). At 400 °C, it can be observed that the size of the grains is small, and their arrangement is extremely disordered. As the temperature increases to 450 °C, the size of grains becomes more uniform. Then, with further increase in the growth temperature, the size of VO<sub>2</sub> grains also increases. A statistical analysis of the grain size of VO<sub>2</sub> films at each temperature [Fig. 3(f)] reveals that the size of VO<sub>2</sub> grains increases with the rise of growth temperature. The basic sputtering process has been known and can be described as some steps: transportation of the species from the target to the substrate; adsorption and diffusion of the species on the substrate; removal of extra species from the substrate; and moving of coating species to the final position to form the film. The diffusion step is controlled mainly by the substrate temperature and may significantly affect the quality of the sputtered film. According to the substrate temperature (*T*) and coating material melting point (*T<sub>m</sub>*), the coating microstructure can be divided into several zones (Thornton's zone model).<sup>53–55</sup> In Zone 1 (or *T*), where  $T/T_m < 0.3$ , since the melting point of VO<sub>2</sub> is approximately 1525 °C,<sup>33</sup> growth temperature of 400 °C falls into this region, under which the atom migration is extremely insufficient due to the low temperature, resulting in smaller grain sizes and poor quality of VO<sub>2</sub> films. For a growth temperature of 450 °C, the  $T/T_m$  is  $\sim 0.295$ , which is close to Zone 2, where  $0.3 < T/T_m < 0.5$ , and growth temperatures of 500, 550, and 600 °C are all within this range. Compared with Zone 1, Zone 2 atoms gain sufficient energy for migration on the substrate surface, and the grains gradually merge and grow larger, forming regularly arranged columnar crystals and a smoother surface. Thus, the VO<sub>2</sub> films grown in Zone 2 have better MIT performance. This is why VO<sub>2</sub> film could achieve good epitaxial growth under growth temperatures as low as 450 °C. Zone 3, where  $0.5 < T/T_m$ , implies that the growth temperature of the VO<sub>2</sub> film needs to be greater than 760 °C. At this point, the grains further grow toward equiaxed grains. However, since current equipment cannot reach such high temperatures, further observation is not feasible.

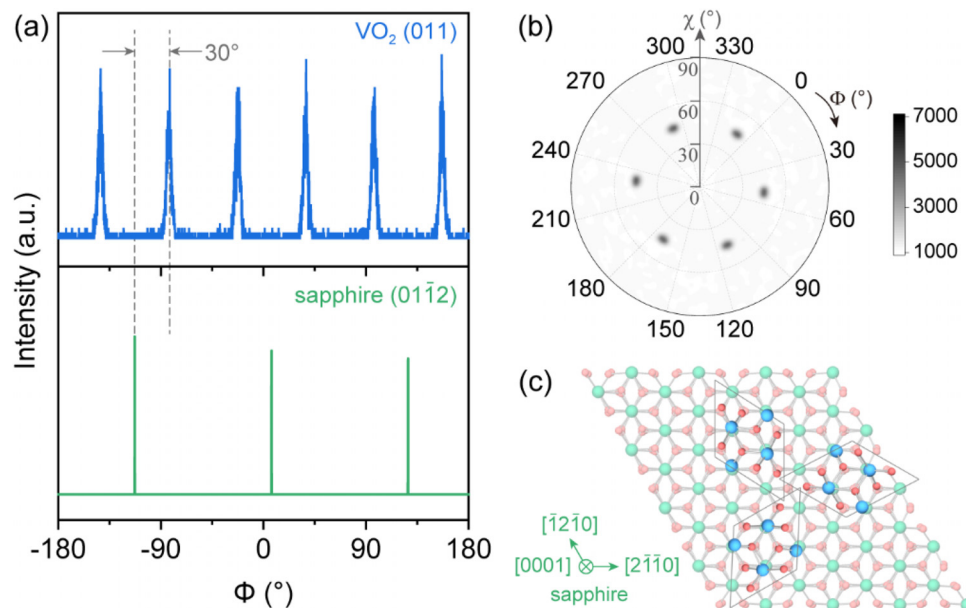
To obtain a high-quality VO<sub>2</sub> epitaxial film based on optimized growth conditions, the epitaxial relationship between the VO<sub>2</sub> and sapphire substrate is also analyzed. XRD  $\varphi$ -scan results for the VO<sub>2</sub> film (011) plane and the sapphire substrate (01 $\bar{1}$ 2) plane are shown in



**FIG. 3.** Morphology of VO<sub>2</sub> films grown under different temperatures. (a)–(e) SEM images of grains of VO<sub>2</sub> films grown under 400, 450, 500, 550, and 600 °C, respectively. Scale bars: 200 nm. (f) Grain sizes of VO<sub>2</sub> films with the variation of growth temperature.

Fig. 4(a). The sapphire substrate exhibits three diffraction peaks spaced at 120° apart, indicating the tri-symmetry of the sapphire (01 $\bar{1}$ 2) plane about the *c*-axis. In contrast, the (011) plane of VO<sub>2</sub> exhibits six diffraction peaks spaced at 60° intervals. In Fig. 4(b), further characterization through pole figure reveals that only six VO<sub>2</sub> diffraction spots are observed within the 0°–90° in-plane range, indicating that from the out-of-plane direction, there is a unique epitaxial orientation of the VO<sub>2</sub> films, while from the in-plane direction, it is neither a single orientation nor polycrystalline. The most plausible explanation, as illustrated in Fig. 4(c), is that the VO<sub>2</sub> crystals (blue) match the sapphire substrate (green) through oxygen atoms, forming a distribution of 120° rotation symmetry in-plane, i.e., three equivalent crystallographic directions with triple rotational symmetry. Consequently, in the XRD  $\varphi$ -scan, the monoclinic VO<sub>2</sub> phase crystal plane, which inherently possesses a double symmetry about the VO<sub>2</sub> [020] crystallographic direction, combined with the in-plane triple rotational distribution, results in six diffraction peaks, which is consistent with observations reported in the literature.<sup>25,56</sup> The results confirm the good epitaxial growth of the VO<sub>2</sub> film on the *c*-plane sapphire substrate.

In conclusion, we realize good epitaxial growth of VO<sub>2</sub> films using reactive magnetron sputtering under a growth temperature as low as 450 °C. Based on the sputtering process model, the O<sub>2</sub> pressure ratio needed for VO<sub>2</sub> growth was calculated precisely. Different stoichiometric vanadium oxides could be prepared according to the theoretical O<sub>2</sub> pressure ratios. Benefiting from the optimized gas condition, the  $\Delta R$  of VO<sub>2</sub> epitaxial film grown at 450 °C exhibits  $10^3$ , while VO<sub>2</sub> epitaxial film grown at 500 °C and above shows a  $\Delta R$  of  $10^4$ , which indicates a high phase transition performance. By analyzing the morphology of VO<sub>2</sub> grains along with Thornton's zone model, the reason



**FIG. 4.** High-resolution XRD analysis between epitaxial the VO<sub>2</sub> film and sapphire substrate. (a) XRD  $\phi$ -scan of VO<sub>2</sub> (011) plane and sapphire (011 $\bar{2}$ ) plane. (b) Pole figure of VO<sub>2</sub> (011) plane. (c) Schematic diagram of epitaxial relation between the VO<sub>2</sub> film and sapphire substrate from out-of-plane direction (blue atoms: V, green atoms: Al, red atoms: O).

why epitaxial growth of VO<sub>2</sub> films can be realized under low growth temperatures was further elucidated. Finally, the epitaxial relationship between the VO<sub>2</sub> film and the c-plane sapphire substrate was determined, confirming the high epitaxial quality. This work provides a more convenient and achievable method for realizing low-cost and large-area growth of VO<sub>2</sub> epitaxial films.

This work was supported by the National Key Technologies R&D Program of China (No. 2021YFA0715302), the National Natural Science Foundation of China (No. 62375054), and the Science and Technology Commission of Shanghai Municipality (Nos. 22ZR1405000 and 21142200200).

## AUTHOR DECLARATIONS

### Conflict of Interest

The authors have no conflicts to disclose.

### Author Contributions

**Chang Liu:** Conceptualization (equal); Data curation (lead); Formal analysis (lead); Investigation (lead); Methodology (lead); Validation (equal); Visualization (lead); Writing – original draft (lead); Writing – review & editing (equal). **Zhi Zheng:** Formal analysis (supporting); Writing – review & editing (equal). **Xing Li:** Formal analysis (supporting); Writing – review & editing (equal). **Yang Wang:** Formal analysis (supporting); Writing – review & editing (equal). **Xiang Dong:** Methodology (supporting). **Gaoshan Huang:** Funding acquisition (equal). **Yongfeng Mei:** Conceptualization (equal); Funding acquisition (equal); Validation (equal); Writing – review & editing (equal).

## DATA AVAILABILITY

The data that support the findings of this study are available from the corresponding author upon reasonable request.

## REFERENCES

- <sup>1</sup>F. Morin, “Oxides which show a metal-to-insulator transition at the Neel temperature,” *Phys. Rev. Lett.* **3**(1), 34 (1959).
- <sup>2</sup>H. Zhang, L. Zhang, D. Mukherjee, Y. Zheng, R. C. Haislmaier, N. Alem, and R. Engel-Herbert, “Wafer-scale growth of VO<sub>2</sub> thin films using a combinatorial approach,” *Nat. Commun.* **6**(1), 8475 (2015).
- <sup>3</sup>M. Liu, A. J. Sternbach, M. Wagner, T. V. Slusar, T. Kong, S. L. Bud’ko, S. Kittiwatanakul, M. Qazilbash, A. McLeod, and Z. Fei, “Phase transition in bulk single crystals and thin films of VO<sub>2</sub> by nanoscale infrared spectroscopy and imaging,” *Phys. Rev. B* **91**(24), 245155 (2015).
- <sup>4</sup>A. Mansingh, R. Singh, and S. Krupanidhi, “Electrical switching in single crystal VO<sub>2</sub>,” *Solid-State Electron.* **23**(6), 649 (1980).
- <sup>5</sup>H. Choi, J. Ahn, J. Jung, T. Noh, and D. Kim, “Mid-infrared properties of a VO<sub>2</sub> film near the metal-insulator transition,” *Phys. Rev. B* **54**(7), 4621 (1996).
- <sup>6</sup>K. Okimura and J. Sakai, “Changes in lattice parameters of VO<sub>2</sub> films grown on c-plane Al<sub>2</sub>O<sub>3</sub> substrates across metal-insulator transition,” *Jpn. J. Appl. Phys., Part 1* **48**(4R), 045504 (2009).
- <sup>7</sup>S. H. Bae, S. Lee, H. Koo, L. Lin, B. H. Jo, C. Park, and Z. L. Wang, “The memristive properties of a single VO<sub>2</sub> nanowire with switching controlled by self-heating,” *Adv. Mater.* **25**(36), 5098 (2013).
- <sup>8</sup>F. Beteille and J. Livage, “Optical switching in VO<sub>2</sub> thin films,” *J. Sol-Gel Sci. Technol.* **13**, 915 (1998).
- <sup>9</sup>S. Rathi, J. Park, I. Lee, J. Baik, K. Yi, and G. Kim, “Unravelling the switching mechanisms in electric field induced insulator-metal transitions in VO<sub>2</sub> nanobeams,” *J. Phys. D: Appl. Phys.* **47**(29), 295101 (2014).
- <sup>10</sup>Y. H. Matsuda, D. Nakamura, A. Ikeda, S. Takeyama, Y. Suga, H. Nakahara, and Y. Muraoka, “Magnetic-field-induced insulator-metal transition in W-doped VO<sub>2</sub> at 500 T,” *Nat. Commun.* **11**(1), 3591 (2020).

- <sup>11</sup>C. Huang, Z. Zhang, S. Ramanathan, and D. Weinstein, "VO<sub>2</sub> phase-transition-based vertical MEMS microactuators," *IEEE Trans. Electron Devices* **66**(10), 4380 (2019).
- <sup>12</sup>D. Torres, T. Wang, J. Zhang, X. Zhang, S. Dooley, X. Tan, H. Xie, and N. Sepúlveda, "VO<sub>2</sub>-based MEMS mirrors," *J. Microelectromech. Syst.* **25**(4), 780 (2016).
- <sup>13</sup>X. Guo, Y. Tan, Y. Hu, Z. Zafar, J. Liu, and J. Zou, "High quality VO<sub>2</sub> thin films synthesized from V<sub>2</sub>O<sub>5</sub> powder for sensitive near-infrared detection," *Sci. Rep.* **11**(1), 21749 (2021).
- <sup>14</sup>Z. Li, Z. Hu, J. Peng, C. Wu, Y. Yang, F. Feng, P. Gao, J. Yang, and Y. Xie, "Ultra-high infrared photoresponse from core-shell single-domain-VO<sub>2</sub>/V<sub>2</sub>O<sub>5</sub> heterostructure in nanobeam," *Adv. Funct. Mater.* **24**(13), 1821 (2014).
- <sup>15</sup>M. Liu, B. Su, Y. V. Kaneti, Z. Chen, Y. Tang, Y. Yuan, Y. Gao, L. Jiang, X. Jiang, and A. Yu, "Dual-phase transformation: Spontaneous self-template surface-patterning strategy for ultra-transparent VO<sub>2</sub> solar modulating coatings," *ACS Nano* **11**(1), 407 (2017).
- <sup>16</sup>K. Liu, C. Cheng, Z. Cheng, K. Wang, R. Ramesh, and J. Wu, "Giant-amplitude, high-work density microactuators with phase transition activated nanolayer bimorphs," *Nano Lett.* **12**(12), 6302 (2012).
- <sup>17</sup>R. Shi, X. Cai, W. Wang, J. Wang, D. Kong, N. Cai, P. Chen, P. He, Z. Wu, and A. Amini, "Single-crystalline vanadium dioxide actuators," *Adv. Funct. Mater.* **29**(20), 1900527 (2019).
- <sup>18</sup>X. Wang, K. Dong, H. S. Choe, H. Liu, S. Lou, K. B. Tom, H. A. Bechtel, Z. You, J. Wu, and J. Yao, "Multifunctional microelectro-opto-mechanical platform based on phase-transition materials," *Nano Lett.* **18**(3), 1637 (2018).
- <sup>19</sup>K. Liu, S. Lee, S. Yang, O. Delaïre, and J. Wu, "Recent progresses on physics and applications of vanadium dioxide," *Mater. Today* **21**(8), 875 (2018).
- <sup>20</sup>S. Zhang, I. S. Kim, and L. J. Lauhon, "Stoichiometry engineering of monoclinic to rutile phase transition in suspended single crystalline vanadium dioxide nanobeams," *Nano Lett.* **11**(4), 1443 (2011).
- <sup>21</sup>M. Borek, F. Qian, V. Nagabushnam, and R. Singh, "Pulsed laser deposition of oriented VO<sub>2</sub> thin films on R-cut sapphire substrates," *Appl. Phys. Lett.* **63**(24), 3288 (1993).
- <sup>22</sup>D. Kim and H. S. Kwok, "Pulsed laser deposition of VO<sub>2</sub> thin films," *Appl. Phys. Lett.* **65**(25), 3188 (1994).
- <sup>23</sup>L. L. Fan, S. Chen, Y. F. Wu, F. H. Chen, W. S. Chu, X. Chen, C. W. Zou, and Z. Y. Wu, "Growth and phase transition characteristics of pure M-phase VO<sub>2</sub> epitaxial film prepared by oxide molecular beam epitaxy," *Appl. Phys. Lett.* **103**(13), 131914 (2013).
- <sup>24</sup>J. W. Tashman, J. H. Lee, H. Paik, J. A. Moyer, R. Misra, J. A. Mundy, T. Spila, T. A. Merz, J. Schubert, D. A. Muller, P. Schiffer, and D. G. Schlom, "Epitaxial growth of VO<sub>2</sub> by periodic annealing," *Appl. Phys. Lett.* **104**(6), 063104 (2014).
- <sup>25</sup>L. Fan, Y. Wu, C. Si, C. Zou, Z. Qi, L. Li, G. Pan, and Z. Wu, "Oxygen pressure dependent VO<sub>2</sub> crystal film preparation and the interfacial epitaxial growth study," *Thin Solid Films* **520**(19), 6124 (2012).
- <sup>26</sup>T.-H. Yang, C. Jin, R. Aggarwal, R. Narayan, and J. Narayan, "On growth of epitaxial vanadium oxide thin film on sapphire (0001)," *J. Mater. Res.* **25**(3), 422 (2010).
- <sup>27</sup>G. Niu, G. Saint-Girons, and B. Vilquin, in *Molecular Beam Epitaxy*, edited by M. Henini (Elsevier, Oxford, 2013), p. 451.
- <sup>28</sup>S. Swann, "Magnetron sputtering," *Phys. Technol.* **19**(2), 67 (1988).
- <sup>29</sup>R. Zhang, X. Li, F. Meng, J. Bi, S. Zhang, S. Peng, J. Sun, X. Wang, L. Wu, and J. Duan, "Wafer-scale epitaxy of flexible nitride films with superior plasmonic and superconducting performance," *ACS Appl. Mater. Interfaces* **13**(50), 60182 (2021).
- <sup>30</sup>E. E. Chain, "The influence of deposition temperature on the structure and optical properties of vanadium oxide films," *J. Vac. Sci. Technol. A* **4**(3), 432 (1986).
- <sup>31</sup>E. E. Chain, "Effects of oxygen in ion-beam sputter deposition of vanadium oxide," *J. Vac. Sci. Technol. A* **5**(4), 1836 (1987).
- <sup>32</sup>Y.-K. Dou, J.-B. Li, M.-S. Cao, D.-Z. Su, F. Rehman, J.-S. Zhang, and H.-B. Jin, "Oxidizing annealing effects on VO<sub>2</sub> films with different microstructures," *Appl. Surf. Sci.* **345**, 232 (2015).
- <sup>33</sup>S. S. Maklakov, V. I. Polozov, S. A. Maklakov, A. D. Mishin, I. A. Ryzhikov, A. L. Trigub, V. A. Amelichev, K. I. Maslakov, and V. N. Kisel, "Post-deposition annealing of thin RF magnetron sputter-deposited VO<sub>2</sub> films above the melting point," *J. Alloys Compd.* **763**, 558 (2018).
- <sup>34</sup>F. Ureña-Begara, A. Crunteanu, and J.-P. Raskin, "Raman and XPS characterization of vanadium oxide thin films with temperature," *Appl. Surf. Sci.* **403**, 717 (2017).
- <sup>35</sup>G. A. Nyberg and R. A. Buhrman, "High optical contrast in VO<sub>2</sub> thin films due to improved stoichiometry," *Thin Solid Films* **147**(2), 111 (1987).
- <sup>36</sup>E. Kusano and J. A. Theil, "Effects of microstructure and nonstoichiometry on electrical properties of vanadium dioxide films," *J. Vac. Sci. Technol. A* **7**(3), 1314 (1989).
- <sup>37</sup>J. Nag, E. A. Payzant, K. L. More, and R. F. Haglund, "Enhanced performance of room-temperature-grown epitaxial thin films of vanadium dioxide," *Appl. Phys. Lett.* **98**(25), 251916 (2011).
- <sup>38</sup>D. Zhang, M. Zhu, Y. Liu, K. Yang, G. Liang, Z. Zheng, X. Cai, and P. Fan, "High performance VO<sub>2</sub> thin films growth by DC magnetron sputtering at low temperature for smart energy efficient window application," *J. Alloys Compd.* **659**, 198 (2016).
- <sup>39</sup>G. Sun, X. Cao, X. Li, S. Bao, N. Li, M. Liang, A. Gloter, H. Gu, and P. Jin, "Low-temperature deposition of VO<sub>2</sub> films with high crystalline degree by embedding multilayered structure," *Sol. Energy Mater. Sol. Cells* **161**, 70 (2017).
- <sup>40</sup>C. Zhang, C. Koughia, O. Güneş, J. Luo, N. Hossain, Y. Li, X. Cui, S.-J. Wen, R. Wong, Q. Yang, and S. Kasap, "Synthesis, structure and optical properties of high-quality VO<sub>2</sub> thin films grown on silicon, quartz and sapphire substrates by high temperature magnetron sputtering: Properties through the transition temperature," *J. Alloys Compd.* **848**, 156323 (2020).
- <sup>41</sup>K. Okimura and Y. Suzuki, "Epitaxial growth of V<sub>2</sub>O<sub>3</sub> thin films on c-plane Al<sub>2</sub>O<sub>3</sub> in reactive sputtering and its transformation to VO<sub>2</sub> films by post annealing," *Jpn. J. Appl. Phys., Part 1* **50**(6R), 065803 (2011).
- <sup>42</sup>S. Berg, H. O. Blom, M. Moradi, C. Nender, and T. Larsson, "Process modeling of reactive sputtering," *J. Vac. Sci. Technol. A* **7**(3), 1225 (1989).
- <sup>43</sup>J. Bohlmark, J. Alami, C. Christou, A. P. Ehasarian, and U. Helmersson, "Ionization of sputtered metals in high power pulsed magnetron sputtering," *J. Vac. Sci. Technol. A* **23**(1), 18 (2005).
- <sup>44</sup>T. E. Sheridan, M. J. Goeckner, and J. Goree, "Pressure dependence of ionization efficiency in sputtering magnetrons," *Appl. Phys. Lett.* **57**(20), 2080 (1990).
- <sup>45</sup>J. E. Greene, "Epitaxial crystal growth by sputter deposition: Applications to semiconductors. Part I," *Crit. Rev. Solid State Mater. Sci.* **11**(1), 47 (1983).
- <sup>46</sup>N. Laegreid and G. Wehner, "Sputtering yields of metals for Ar<sup>+</sup> and Ne<sup>+</sup> ions with energies from 50 to 600 eV," *J. Appl. Phys.* **32**(3), 365 (1961).
- <sup>47</sup>J. A. Theil, E. Kusano, and A. Rockett, "Vanadium reactive magnetron sputtering in mixed Ar/O<sub>2</sub> discharges," *Thin Solid Films* **298**(1-2), 122 (1997).
- <sup>48</sup>H. Yu, Y. Jiang, T. Wang, Z. Wu, J. Yu, and X. Wei, "Modeling for calculation of vanadium oxide film composition in reactive-sputtering process," *J. Vac. Sci. Technol. A* **28**(3), 466 (2010).
- <sup>49</sup>P. T. P. Le, S. Huang, M. D. Nguyen, J. E. ten Elshof, and G. Koster, "Tuning the metal insulator transition of vanadium dioxide on oxide nanosheets," *Appl. Phys. Lett.* **119**(8), 081601 (2021).
- <sup>50</sup>M. K. Sohn, H. Singh, E.-M. Kim, G. S. Heo, S. W. Choi, D. G. Phyun, and D. J. Kang, "Strain-dependent phase-change devices based on vanadium dioxide thin films on flexible glass substrates," *Appl. Phys. Lett.* **120**(17), 173503 (2022).
- <sup>51</sup>X. Gao, C. M. M. Rosário, and H. Hilgenkamp, "Multi-level operation in VO<sub>2</sub>-based resistive switching devices," *AIP Adv.* **12**(1), 015218 (2022).
- <sup>52</sup>Y. Cui and S. Ramanathan, "Substrate effects on metal-insulator transition characteristics of rf-sputtered epitaxial VO<sub>2</sub> thin films," *J. Vac. Sci. Technol. A* **29**(4), 041502 (2011).
- <sup>53</sup>P. J. Kelly and R. D. Arnell, "Magnetron sputtering: A review of recent developments and applications," *Vacuum* **56**(3), 159 (2000).
- <sup>54</sup>T. A. Thornton, "Influence of apparatus geometry and deposition conditions on the structure and topography of thick sputtered coatings," *J. Vac. Sci. Technol.* **11**(4), 666 (1974).
- <sup>55</sup>J. A. Thornton, "High rate thick film growth," *Annu. Rev. Mater. Sci.* **7**(1), 239 (1977).
- <sup>56</sup>Y. Guo, X. Sun, J. Jiang, B. Wang, X. Chen, X. Yin, W. Qi, L. Gao, L. Zhang, and Z. Lu, "A reconfigurable remotely epitaxial VO<sub>2</sub> electrical heterostructure," *Nano Lett.* **20**(1), 33 (2020).